

Second-order Optical Response from First Principles

S. Sharma* and C. Ambrosch-Draxl

Institute for Theoretical Physics, Karl-Franzens-Universität Graz, Universitätsplatz 5, A-8010 Graz, Austria.

(Dated: December 20, 2018)

We present a full formalism for the calculation of the linear and second-order optical response for semiconductors and insulators. The expressions for the optical susceptibilities are derived within perturbation theory. As a starting point a brief background of the single and many particle Hamiltonians and operators is provided. As an example we report calculations of the linear and nonlinear optical properties of the mono-layer InP/GaP (110) superlattice. The features in the linear optical spectra are identified to be coming from various band combinations. The main features in the second-order optical spectra are analyzed in terms of resonances of peaks in linear optical spectra. With the help of the strain corrected effective-medium-model the interface selectivity of the second-order optical properties is highlighted.

PACS numbers: 61.50A, 42.65K, 61.50K, 78.66H

I. INTRODUCTION

A material interacting with the intense light of a laser beam responds in a "nonlinear fashion". Consequences of this are a number of peculiar phenomena, including the generation of optical frequencies that are initially absent. This effect allows the production of laser light at wave lengths normally unattainable by conventional laser techniques. So the application of nonlinear optics (NLO) range from basic research to spectroscopy, telecommunications and astronomy. Second harmonic generation (SHG), in particular, corresponds to the appearance of a frequency component in the laser beam that is exactly twice the input one. SHG has great potential as a characterization tool for materials, because of its sensitivity to symmetry. Today SHG is widely applied for studying the surfaces and interfaces because it requires an inversion asymmetric material. For materials with bulk inversion symmetry SHG is only allowed at surfaces and interfaces. This makes SHG a powerful surface selective technique. SHG in conjunction with Kerr and Faraday rotation¹ is used as an excellent tool for studying magnetic surfaces. In case of embedded interfaces this technique gains extra weight when an intense laser is used which is capable of penetrating deep into the material and no direct contact with the sample is needed.

In the case of linear optical transitions an electron absorbs a photon from the incoming light and makes a transition to the next higher unoccupied allowed state. When this electron relaxes it emits a photon of frequency less than or equal to the frequency of the incident light (Fig. 1(a)). SHG on the other hand is a two photon process where this excited electron absorbs another photon of same frequency and makes a transition to yet another allowed state at higher energy. This electron when falling back to its original state emits a photon of a frequency which is two times that of the incident light (Fig. 1(b)). This results in the frequency doubling in the output.

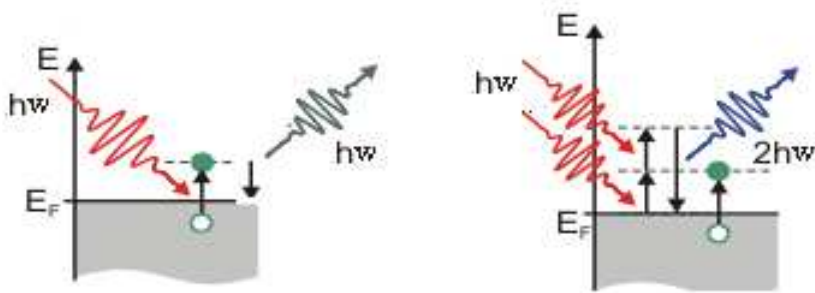


FIG. 1: Schematic representation of a (a) linear optical transition and (b) second harmonic generation.

In order to extend the use of NLO for understanding the properties of surfaces and interfaces and for extracting maximal information from such measurements for non centero-symmetric materials, a more quantitative theoretical analysis is required. The calculation of the SHG susceptibility from first principles is an important but difficult task. The major work in this direction for semiconductors can be found in Refs. 2,3,4,5 and for metals in Refs. 6,7,8,9 and references there in. In this work, we present the formalism for calculating the second order susceptibility $\chi^{(2)}(2\omega, \omega, \omega)$ for non magnetic semiconductors and insulators, within the independent particle approximation. The expressions formulated are amenable for numerical calculations using any band structure method and are computationally more efficient¹⁰ than the previously presented expressions.^{2,3,4,5}

As an example, we present the linear and nonlinear optical properties of a InP/GaP superlattice (SL). Semiconducting strained SLs are potential materials for applications in optical communications involving switching, amplification and signal processing. In particular III-V semiconductor hetero-structures and SLs have attracted a great deal of interest mainly due to the possibility of tailoring band gaps and band structures by variation of simple parameters like superlattice period, growth direction and substrate material. Much of the theoretical work done to understand the physical properties of SLs has been largely concerned with the understanding of the electronic band structure. For example, the effect of strain on the band gap, the band offset problem and the possibilities of engineering it as well as the interface energy and band structure have been studied.^{11,12,13,14,15,16,17,18,19,20,21,22} The major theoretical work in the direction of NLO properties was done by Ghahramani *et al.*^{23,24,25,26} They employed the non-self consistent linear-combination-of-Gaussian-orbitals (LCGO) method to calculate the band structures and optical properties of SLs. As an example, we present a fully self-consistent calculation of the nonlinear optical properties of the mono-layer InP/GaP (110) superlattice (SL). The structure in the linear optical spectra is identified from the band structure of the material. The features in the second-order optical response are further analyzed in terms of resonances of the peaks in the linear optical spectra. With use of the strain corrected effective-medium-model (SCEMM),¹⁰ and we identify the features in the optical spectra of InP/GaP coming from the SL formation.

The paper is arranged in the following manner. In Section II we present the detailed formalism for calculating the SHG susceptibility. Section III deals with the linear and second-order optical response of an InP/GaP SL.

II. FORMALISM

The aim of the present work is to obtain the expressions for the optical response of a material. The effect of the electric field vector $\mathbf{E}(\omega)$ of the incoming light is to polarize the material. This polarization can be calculated using the following relation:

$$\mathbf{P}^a(\omega) = \chi_{ab}^{(1)} \cdot \mathbf{E}^b(\omega) + \chi_{abc}^{(2)} \cdot \mathbf{E}^b(\omega) \cdot \mathbf{E}^c(\omega) + \dots \quad (1)$$

In this expression $\chi^{(1)}$ is the linear optical susceptibility and $\chi^{(2)}$ is the second order optical susceptibility. The higher order terms can also be calculated but in the present work we are only interested up to the second-order optical response. The formulae for calculating the SHG susceptibility, $\chi^{(2)}(2\omega, \omega, \omega)$, have been presented before.^{2,3,4,5} In the present work we provide the detailed formalism. Before deriving the expressions for calculating the SHG susceptibility using perturbation theory, a brief background of the single and many particle Hamiltonians and operators is needed. This is presented in the following two sections.

A. THE HAMILTONIANS

The optical response is treated within the independent particle approximation and the Hamiltonian in a.u. (i.e. $\hbar = m = e = 1$) is written as

$$H(t) = \sum_i \frac{(\mathbf{p}_i - \mathbf{K}(t))^2}{2} + V(\mathbf{x}_i) \quad (2)$$

The subscript i labels the electrons in the crystal at position \mathbf{x}_i . \mathbf{p} is the momentum operator given by $\mathbf{p}_i = -i\nabla_i$. $V(\mathbf{x})$ is the effective periodic crystal potential. $\mathbf{K}(t) = \mathbf{A}(t)/c$ where $\mathbf{A}(t)$ is the vector potential of the external applied field. The macroscopic electric field is given by $\mathbf{E}(t) = -\dot{\mathbf{A}}(t)/c$. In the long wavelength limit the variation of this field over the distance of the lattice spacing is neglected. Eq. (2) can be separated into a time independent (which may be implicitly time dependent) and explicitly time dependent parts as

$$H = H_0 + H_1 + H_2 \quad (3)$$

with

$$H_0 = \sum_i H_{0i} = \frac{1}{2} \sum_i \mathbf{p}_i^2 + V(\mathbf{x}_i) \quad (4)$$

$$H_1(t) = -\mathbf{K}(t) \sum_i \mathbf{p}_i \quad (5)$$

$$H_2(t) = \frac{1}{2} N \mathbf{K}^2(t) \quad (6)$$

N is the total number of electrons in the volume Ω of the crystal. In the long wavelength limit H_2 only introduces a time dependent phase factor for the wave functions and hence can be neglected. H_1 can be treated as a perturbation. The eigenstates of H_0 are given by

$$\begin{aligned} H_0 \psi_n(\mathbf{k}, \mathbf{x}) &= \omega_n(\mathbf{k}) \psi_n(\mathbf{k}, \mathbf{x}) \\ \psi_n(\mathbf{k}, \mathbf{x}) &= \Omega^{-1/2} u_n(\mathbf{k}, \mathbf{x}) e^{i\mathbf{k} \cdot \mathbf{x}} \end{aligned} \quad (7)$$

Next we consider the time dependent single particle Hamiltonian $H(t) = \frac{1}{2}(\mathbf{p} - \mathbf{K}(t))^2 + V(\mathbf{x})$. The instantaneous eigenstates of this Hamiltonian are

$$\bar{\psi}_n(\mathbf{k}, \mathbf{x}) = \Omega^{-1/2} u_n(\mathbf{k} + \mathbf{K}(t), \mathbf{x}) e^{i\mathbf{k} \cdot \mathbf{x}} \quad (8)$$

satisfying

$$H(t) \bar{\psi}_n(\mathbf{k}, \mathbf{x}) = \omega_n(\mathbf{k} + \mathbf{K}(t)) \bar{\psi}_n(\mathbf{k}, \mathbf{x}). \quad (9)$$

$\bar{\psi}_n(\mathbf{k}, \mathbf{x})$ is implicitly time dependent via $\mathbf{K}(t)$. If an orthonormal set $\bar{\psi}_n(\mathbf{k}, \mathbf{x})$ satisfies Eq. (9) at time t , then the same equation is satisfied at time $t + dt$ if

$$i\hbar \frac{d}{dt} \bar{\psi}_n(\mathbf{k}, \mathbf{x}) = \sum_m \bar{\psi}_m(\mathbf{k}, \mathbf{x}) \mu_{mn}(\mathbf{k}, t) \mathbf{E}(t) \quad (10)$$

for each n . If $\omega_l(\mathbf{k} + \mathbf{K}) = \omega_n(\mathbf{k} + \mathbf{K})$ then

$$\mathbf{E}(t) \cdot \mathbf{V}_{mn}(\mathbf{k}, t) = 0. \quad (11)$$

It can be shown³ that the above conditions require:

$$\mu_{mn}(\mathbf{k} + \mathbf{K}, t) = \frac{\mathbf{V}_{mn}(\mathbf{k}, t)}{i\omega_{mn}(\mathbf{k} + \mathbf{K})} \quad (12)$$

where

$$V_{mn}(\mathbf{k}, t) = \int \bar{\psi}_m^*(\mathbf{k}, \mathbf{x}) e^{-i\mathbf{k} \cdot \mathbf{x}} [-i\nabla] \bar{\psi}_n(\mathbf{k}, \mathbf{x}) e^{i\mathbf{k} \cdot \mathbf{x}} d\mathbf{x} \quad (13)$$

B. THE OPERATORS IN SECOND QUANTIZATION

We now introduce Fermionic raising and lowering operators a_n^+ and a_n satisfying the anti-commutation relations $\{a_n^+, a_m^+\} = \{a_n, a_m\} = 0$ and $\{a_n^+, a_m\} = \delta_{nm}$. Similar commutation relations are satisfied by b_n^+ and b_n which are Fermionic raising and lowering operators, implicitly dependent on time via the wave function. The Hamiltonians in the second quantized representation are

$$H_0 = \sum_{n\mathbf{k}} \omega_n(\mathbf{k}) a_{n\mathbf{k}}^+ a_{n\mathbf{k}} \quad (14)$$

$$H(t) = \sum_{n\mathbf{k}} \omega_n(\mathbf{k} + \mathbf{K}) b_{n\mathbf{k}}^+ b_{n\mathbf{k}} \quad (15)$$

A unitary transformation operator can be used for going from the implicitly time dependent operators b_n and b_n^+ to time independent operators a_n and a_n^+ as

$$\begin{aligned} a_n &= U b_n U^+ \\ a_n^+ &= U b_n^+ U^+ \end{aligned} \quad (16)$$

Here

$$\begin{aligned} U &= \sum_S |S\rangle \langle \bar{S}| \\ U^+ &= \sum_S |\bar{S}\rangle \langle S| \end{aligned} \quad (17)$$

such that $|S\rangle$ are states given by Eq. (7), $|\bar{S}\rangle$ are states given by Eq. (8) and the sum runs over all the states. The importance of such a transformation will become clear in the next section (see for example Eq 25 and the discussion after it). Since our final aim is to calculate the linear and nonlinear optical response of the material another useful operator is the current density operator \mathbf{J} which is given by

$$\mathbf{J} = \frac{1}{\Omega} \sum_i \mathbf{p}_i - \mathbf{K}(t) \quad (18)$$

$$= \frac{d\mathbf{P}}{dt} = \frac{1}{\Omega} \sum_{nm\mathbf{k}} b_{n\mathbf{k}}^+ b_{m\mathbf{k}} \mathbf{V}_{nm}(\mathbf{k} + \mathbf{K})$$

$$\mathbf{J}' = \sum_{nm\mathbf{k}} a_{n\mathbf{k}}^+ a_{m\mathbf{k}} \mathbf{V}_{nm}(\mathbf{k} + \mathbf{K}) \quad (19)$$

here \mathbf{P} , the effective polarization of the material given by Eq. (1), and in second quantization this operator can be written as

$$\begin{aligned} \mathbf{P} &= \frac{1}{\Omega} \sum_{nm\mathbf{k}} b_{n\mathbf{k}}^+ b_{m\mathbf{k}} \mu_{nm}(\mathbf{k}, t) \\ \mathbf{P}' &= \frac{1}{\Omega} \sum_{nm\mathbf{k}} a_{n\mathbf{k}}^+ a_{m\mathbf{k}} \mu_{nm}(\mathbf{k}, t) \end{aligned} \quad (20)$$

C. THE PERTURBATION APPROACH

1. SCHRÖDINGER TO INTERACTION PICTURE

With the above information now we are ready to study the dynamics of a many-particle system described by the density matrix ρ , which is specified by the following equation of motion

$$i\dot{\rho} = [H, \rho] \quad (21)$$

Working with the transformed operators $\rho' = U\rho U^+$ the equation of motion becomes

$$i\dot{\rho}' = [H' + H'_d, \rho'] \quad (22)$$

where

$$\begin{aligned} H'_d &= -\Omega \mathbf{P}' \mathbf{E}(t) \\ &= -\sum_{nm\mathbf{k}} a_{n\mathbf{k}}^+ a_{m\mathbf{k}} \mu_{nm}(\mathbf{k}, t) \mathbf{E}(t) \end{aligned} \quad (23)$$

$$\begin{aligned} H' &= U H U^+ \\ &= \sum_{n\mathbf{k}} \omega_n(\mathbf{k} + \mathbf{K}) a_{n\mathbf{k}}^+ a_{n\mathbf{k}} \end{aligned} \quad (24)$$

In this equation a_n^+ and a_n are time independent and hence the commutators of H' at two different times vanish.

Until now we have been working in the Schrödinger picture. Now we change to the interaction picture, because the equation of motion Eq. (21) involving total Hamiltonian simplifies to the form given by Eq. (27), where only the perturbation term of the Hamiltonian H_d , is involved. This can be done by the use of the following relations

$$\frac{dW(t)}{dt} = \exp \left[i \int_{-\infty}^t H'(t') dt' \right] \quad (25)$$

$$\begin{aligned} \tilde{\rho} &= W \rho' W^+ \\ \tilde{a}_{m\mathbf{k}} &= W a_{m\mathbf{k}} W^+ \\ \tilde{a}_{m\mathbf{k}}(t) &= a_{m\mathbf{k}} e^{-i\nu_m(\mathbf{k}, t)} \\ \tilde{H}_d = W H'_d W^+ &= - \sum_{nm\mathbf{k}} \tilde{a}_{n\mathbf{k}}^+ \tilde{a}_{m\mathbf{k}} \mu_{nm}(\mathbf{k}, t) \mathbf{E}(t). \end{aligned} \quad (26)$$

Here $\nu_m(\mathbf{k}, t) = \int_{-\infty}^t \omega_m(\mathbf{k} + \mathbf{K}(t')) dt'$. Eq. (21) now becomes

$$i\dot{\tilde{\rho}} = [\tilde{H}_d, \tilde{\rho}] \quad (27)$$

Integrating this equation we get

$$\begin{aligned} \tilde{\rho} &= \rho_0 + \frac{1}{i} \int_{-\infty}^t [\tilde{H}'_d(t'), \rho_0] dt' \\ &+ \frac{1}{(i)^2} \int_{-\infty}^t \int_{-\infty}^{t'} [\tilde{H}_d(t'), [\tilde{H}'_d(t''), \rho_0]] dt' dt'' \dots \end{aligned} \quad (28)$$

2. EXPECTATION VALUES OF OPERATORS

Our main interest lies in the single particle operators like

$$\begin{aligned} \Theta &= \sum_{nm\mathbf{k}} a_{n\mathbf{k}}^+ a_{m\mathbf{k}} \Theta_{nm}(\mathbf{k}) = \sum_{nm\mathbf{k}} b_{n\mathbf{k}}^+ b_{m\mathbf{k}} \bar{\Theta}_{nm}(\mathbf{k}) \\ \Theta' &= \sum_{nm\mathbf{k}} a_{n\mathbf{k}}^+ a_{m\mathbf{k}} \bar{\Theta}_{nm}(\mathbf{k}) \\ \tilde{\Theta} &= \sum_{nm\mathbf{k}} \tilde{a}_{n\mathbf{k}}^+ \tilde{a}_{m\mathbf{k}} \Theta_{nm}(\mathbf{k} + \mathbf{K}) \end{aligned} \quad (29)$$

The expectation value of any single particle operator Θ can be calculated using the relation

$$\langle \Theta \rangle = \text{Tr}(\rho \Theta) = \text{Tr}(\rho' \Theta') = \text{Tr}(\rho_0 \hat{\Theta}) \quad (30)$$

where $\hat{\Theta}$ is

$$\begin{aligned} \hat{\Theta} &= \tilde{\Theta}(t) + \frac{1}{i} \int_{-\infty}^t [\tilde{\Theta}(t) \tilde{H}_d(t')] dt' \\ &+ \frac{1}{(i)^2} \int_{-\infty}^t \int_{-\infty}^{t'} [[\tilde{\Theta}(t), \tilde{H}_d(t')], \tilde{H}_d(t'')] dt' dt'' + \dots \end{aligned} \quad (31)$$

Using the following properties of the trace

$$\begin{aligned} \text{Tr}(\rho_0 a_{n\mathbf{k}}^+ a_{m\mathbf{k}}) &= \delta_{nm} f_n(\mathbf{k}) \\ \text{Tr}(\rho_0 [a_{n\mathbf{k}}^+ a_{m\mathbf{k}} a_{p\mathbf{k}'}^+ a_{q\mathbf{k}'}]) &= \delta_{\mathbf{k}, \mathbf{k}'} \delta_{nq} \delta_{mp} f_{nm}(\mathbf{k}) \end{aligned} \quad (32)$$

and combining Eqs. (28), (30) and (31) the first terms becomes

$$\langle \Theta \rangle_{(0)} = \sum_{nk} \Theta_{nn}(\mathbf{k} + \mathbf{K}, t) f_n(\mathbf{k}) \quad (33)$$

and the second term is

$$\begin{aligned} \langle \Theta \rangle_{(1)} &= i \sum_{nm\mathbf{k}} f_{nm}(\mathbf{k}) \Theta_{nm}(\mathbf{k}, t) e^{i\nu_{mn}(\mathbf{k}, t)} \\ &\times \int_{-\infty}^t e^{i\nu_{mn}(\mathbf{k}, t')} \mu_{mn}(\mathbf{k}, t') \mathbf{E}(t') dt' \end{aligned} \quad (34)$$

The higher order terms can be written in a similar manner. Taking $\mathbf{E}(t) = \sum_{\beta} \mathbf{E}(\omega_{\beta}) e^{-i\omega_{\beta}t}$, using the following identity

$$e^{S(t)} L(t) = \frac{d}{dt} \left[e^{S(t)} \frac{L(t)}{\dot{S}(t)} \right] - e^{S(t)} \frac{d}{dt} \left[\frac{L(t)}{\dot{S}(t)} \right] \quad (35)$$

and substituting $S(t) = i(\nu_{mn} - \omega_{\beta}t)$, $L(t) = \mu_{mn}^b$ and $\dot{S} = i(\omega_{mn} - \omega_{\beta})$ in Eq. (34) we get

$$\begin{aligned} \langle \Theta \rangle_{(1)} &= i \sum_{nm\mathbf{k}} f_{nm}(\mathbf{k}) \Theta_{nm}(\mathbf{k}, t) e^{i\nu_{mn}(\mathbf{k}, t)} \\ &\times \left\{ e^{i(\nu_{mn}(\mathbf{k}, t) - \omega_{\beta}t)} \frac{\mu_{mn}^b(\mathbf{k}, t)}{i(\omega_{mn}(\kappa) - \omega_{\beta})} \right. \\ &\left. + i \int_{-\infty}^t e^{i(\nu_{mn}(\mathbf{k}, t') - \omega_{\beta}t')} \frac{\delta}{\delta \kappa'_c} \left[\frac{\mu_{mn}^b(\mathbf{k}, t')}{(\omega_{mn}(\kappa') - \omega_{\beta})} \right] \mathbf{E}^c(t') dt' \right\} \mathbf{E}^b(\omega_{\beta}) \end{aligned} \quad (36)$$

Now expanding $E(t')$ in frequency components $E(\omega)$ and using Eq. (35) for integrating the right side of Eq. (36) one can write $\langle \Theta \rangle_{(1)} = \langle \Theta \rangle_{(1,0)} + \langle \Theta \rangle_{(1,1)} + \dots$ where

$$\begin{aligned} \langle \Theta \rangle_{(1,0)} &= \sum_{nm\mathbf{k}} f_{nm}(\mathbf{k}) \Theta_{nm}(\mathbf{k}, t) \frac{\mu_{mn}^b(\mathbf{k}, t)}{(\omega_{mn} - \omega_{\beta})} \times \\ &e^{-i\omega_{\beta}t} \mathbf{E}^b(\omega_{\beta}) \end{aligned} \quad (37)$$

$$\begin{aligned} \langle \Theta \rangle_{(1,1)} &= i \sum_{nm\mathbf{k}} f_{nm}(\mathbf{k}) \Theta_{nm}(\mathbf{k}, t) \frac{1}{\omega_{mn} - \omega_{\beta} - \omega_{\gamma}} \times \\ &\frac{\delta}{\delta \kappa^c} \left[\frac{\mu_{mn}^b(\mathbf{k}, t)}{\omega_{mn} - \omega_{\beta}} \right] e^{-i(\omega_{\beta} + \omega_{\gamma})t} \mathbf{E}^b(\omega_{\beta}) \mathbf{E}^c(\omega_{\gamma}) \end{aligned} \quad (38)$$

and

$$\begin{aligned} \langle \Theta \rangle_{(2,0)} &= \sum_{nm\mathbf{k}} \frac{1}{\omega_{mn} - \omega_{\beta} - \omega_{\gamma}} \left\{ \frac{f_{nl} \Theta_{nm}(\mathbf{k}, t) \mu_{ml}^b \mu_{ln}^c}{\omega_{ln} - \omega_{\gamma}} + \right. \\ &\left. \frac{f_{ml} \theta_{nm} \mu_{ml}^c \mu_{ln}^b}{\omega_{ml} - \omega_{\gamma}} \right\} e^{-i(\omega_{\beta} + \omega_{\gamma})t} \mathbf{E}^b(\omega_{\beta}) \mathbf{E}^c(\omega_{\gamma}) \end{aligned} \quad (39)$$

D. LINEAR AND SECOND ORDER SUSCEPTIBILITY

Up to this point the things have been most general. Now in order to find the linear and non linear susceptibility Θ is replaced by the polarization operator \mathbf{P} . Expanding Eq. (18) and Eq. (20) in the powers of the electric field we get

$$\begin{aligned} \langle \mathbf{P} \rangle &= \langle \mathbf{P} \rangle_I + \langle \mathbf{P} \rangle_{II} + \dots \\ \langle \mathbf{J}_A \rangle &= \langle \mathbf{J}_A \rangle_I + \langle \mathbf{J}_A \rangle_{II} + \dots \end{aligned} \quad (40)$$

where

$$\begin{aligned} \langle \mathbf{P}^a \rangle_I &= \chi_{ab}^{(1)}(-\omega_{\beta}, \omega_{\beta}) e^{-i\omega_{\beta}t} \mathbf{E}^b(\omega_{\beta}) \\ \langle \mathbf{P}^a \rangle_{II} &= \chi_{abc}^{(II)}(-\omega_{\beta}, -\omega_{\gamma}, \omega_{\beta}, \omega_{\gamma}) e^{-i(\omega_{\beta} + \omega_{\gamma})t} \mathbf{E}^b(\omega_{\beta}) \mathbf{E}^c(\omega_{\gamma}) \end{aligned} \quad (41)$$

and

$$\begin{aligned} \langle \mathbf{J}_A \rangle_I &= \sigma_{ab}^{(1)}(-\omega_\beta, \omega_\beta) e^{-i\omega_\beta t} \mathbf{E}^b(\omega_\beta) \\ \langle \mathbf{J}_A \rangle_{II} &= \sigma_{abc}^{(II)}(-\omega_\beta, -\omega_\gamma, \omega_\beta, \omega_\gamma) e^{-i(\omega_\beta + \omega_\gamma)t} \mathbf{E}^b(\omega_\beta) \mathbf{E}^c(\omega_\gamma). \end{aligned} \quad (42)$$

For clean semiconductors with filled bands the conductivity $\sigma^{(1)}$ is zero and only \mathbf{P}_I contributes to the linear term, whereas to the second-order term both, \mathbf{P}_{II} and \mathbf{J}_{II} , contribute. Now substituting $\Theta = \mathbf{P}^a$ in Eq. (37) we get the expression for the linear susceptibility

$$\chi_{ab}^{(1)}(-\omega, \omega) = \frac{1}{\Omega} \sum_{nm\mathbf{k}} f_{nm}(\mathbf{k}) \frac{\mathbf{r}_{nm}^a(\mathbf{k}) \mathbf{r}_{mn}^b(\mathbf{k})}{\omega_{mn}(\mathbf{k}) - \omega} = \frac{\epsilon_{ab}(\omega) - \delta_{ab}}{4\pi} \quad (43)$$

Here $\epsilon^{ab}(\omega)$ is the ab component of the dielectric tensor, and \mathbf{r}_{nm} are the position matrix elements given by

$$\begin{aligned} \mathbf{r}_{nm} &= \mu_{nm} = \frac{\mathbf{V}_{nm}(\mathbf{k}, t)}{i\omega_{nm}(\mathbf{k} + \mathbf{K})} & \text{if } \omega_n \neq \omega_m \\ \mathbf{r}_{nm} &= 0 & \text{if } \omega_n = \omega_m. \end{aligned} \quad (44)$$

Similarly, substituting $\Theta = \mathbf{P}^a$ in Eqs. (38) and (39) and using the following identity

$$\chi_{abc}^{(2)}(-\omega_\beta, -\omega_\gamma, \omega_\beta, \omega_\gamma) = \chi_{abc}^{(II)}(-\omega_\beta, -\omega_\gamma, \omega_\beta, \omega_\gamma) + \frac{\sigma_{abc}^{(II)}(-\omega_\beta, -\omega_\gamma, \omega_\beta, \omega_\gamma)}{\omega_\beta + \omega_\gamma} \quad (45)$$

we get after some rearrangement of the terms^{3,10} the following contributions to the SHG susceptibility: the interband transitions $\chi_{\text{inter}}(2\omega, \omega, \omega)$, the intraband transitions $\chi_{\text{intra}}(2\omega, \omega, \omega)$ and the modulation of interband terms by intraband terms $\chi_{\text{mod}}(2\omega, \omega, \omega)$:

$$\begin{aligned} \chi_{\text{inter}}^{abc}(2\omega, \omega, \omega) &= \frac{1}{\Omega} \sum'_{nml} \sum_{\mathbf{k}} W_{\mathbf{k}} \left\{ \frac{2\mathbf{r}_{nm}^a \{ \mathbf{r}_{ml}^b \mathbf{r}_{ln}^c \}}{(\omega_{ln} - \omega_{ml})(\omega_{mn} - 2\omega)} \right. \\ &\quad \left. - \frac{1}{(\omega_{mn} - \omega)} \left[\frac{\mathbf{r}_{lm}^c \{ \mathbf{r}_{mn}^a \mathbf{r}_{nl}^b \}}{(\omega_{nl} - \omega_{mn})} - \frac{\mathbf{r}_{nl}^b \{ \mathbf{r}_{lm}^c \mathbf{r}_{mn}^a \}}{(\omega_{lm} - \omega_{mn})} \right] \right\} \end{aligned} \quad (46)$$

$$\begin{aligned} \chi_{\text{intra}}^{abc}(2\omega, \omega, \omega) &= \frac{1}{\Omega} \sum_{\mathbf{k}} W_{\mathbf{k}} \left\{ \sum'_{nml} \frac{1}{\omega_{mn}^2(\omega_{mn} - \omega)} [\omega_{ln} \mathbf{r}_{nl}^b \{ \mathbf{r}_{lm}^c \mathbf{r}_{mn}^a \} - \omega_{ml} \mathbf{r}_{lm}^c \{ \mathbf{r}_{mn}^a \mathbf{r}_{nl}^b \}] \right. \\ &\quad \left. - 8i \sum'_{nm} \frac{1}{\omega_{mn}^2(\omega_{mn} - 2\omega)} \mathbf{r}_{nm}^a \{ \mathbf{r}_{ml}^b \mathbf{r}_{ln}^c \} + 2 \sum'_{nml} \frac{\mathbf{r}_{nm}^a \{ \mathbf{r}_{ml}^b \mathbf{r}_{ln}^c \} (\omega_{ml} - \omega_{ln})}{\omega_{mn}^2(\omega_{mn} - 2\omega)} \right\} \end{aligned} \quad (47)$$

$$\begin{aligned} \chi_{\text{mod}}^{abc}(2\omega, \omega, \omega) &= \frac{1}{2\Omega} \sum_{\mathbf{k}} W_{\mathbf{k}} \left\{ \sum'_{nml} \frac{1}{\omega_{mn}^2(\omega_{mn} - \omega)} [\omega_{nl} \mathbf{r}_{lm}^a \{ \mathbf{r}_{mn}^b \mathbf{r}_{nl}^c \} - \omega_{lm} \mathbf{r}_{nl}^a \{ \mathbf{r}_{lm}^b \mathbf{r}_{mn}^c \}] \right. \\ &\quad \left. - i \sum_{nm} \frac{\mathbf{r}_{nm}^a \{ \mathbf{r}_{mn}^b \Delta_{mn}^c \}}{\omega_{mn}^2(\omega_{mn} - \omega)} \right\} \end{aligned} \quad (48)$$

$W_{\mathbf{k}}$ is the weight of the \mathbf{k} point, n denotes the valence states, m the conduction states and l denotes all states ($l \neq m, n$). We have used these expressions to calculate the total susceptibility in the following example.

III. EXAMPLE

As an example we present the linear and nonlinear optical spectra of an InP/GaP (110) superlattice. This material is a mono-layer SL in (110) direction with GaP grown on top of an InP substrate. The zz component of the linear frequency dependent dielectric function is given in Fig. 2(a). $\epsilon_2^{zz}(\omega)$ has major peaks at 2.3eV (B), 4eV (D) and 5.5eV (F) and minor peaks at 1eV (A), 2.75eV (C), 4.5eV (E) and 6.5eV (G). These peaks in the linear optical spectra can

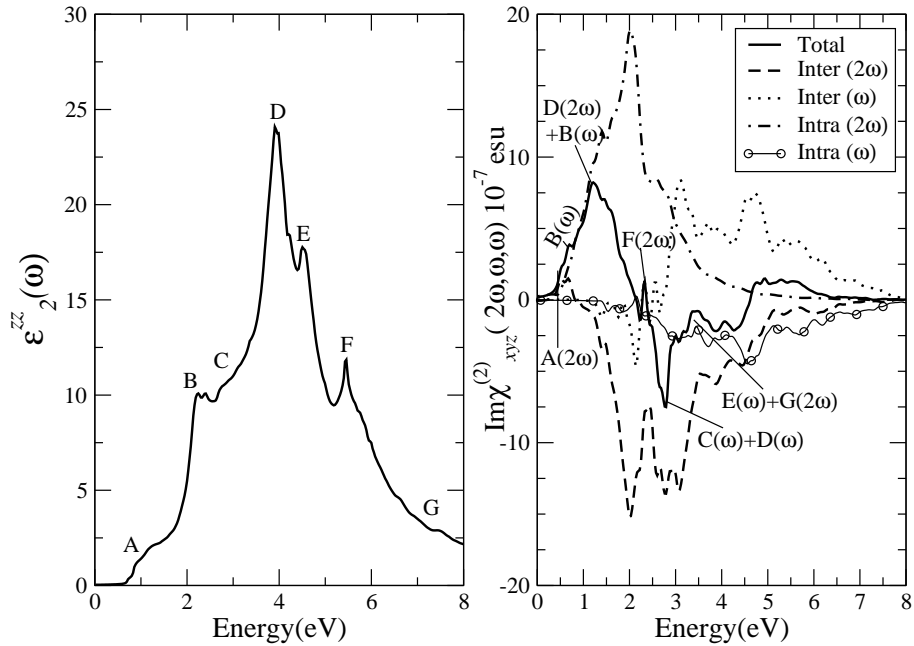


FIG. 2: (a) Imaginary part of the zz component of the linear dielectric tensor. (b) Second-order susceptibility $\text{Im}[\chi_{xyz}^{(2)}(2\omega, \omega, \omega)]$ (solid line) and different contributions to it: the “ 2ω interband term” (dashed line), the “ ω interband term” (dotted line), the “ 2ω intraband term” (dash dotted line) and the “ ω intraband term” (circle thin line)

be identified from the band structure. The calculated band structure along certain symmetry directions is given in Fig. 3. It can be noted from the band structure plot that InP/GaP is a direct band gap (E_G) material. The calculated band gap using the local density approximation (LDA) is $E_G = 0.6\text{eV}^{27}$. As can be seen from the Eq. (43), in order to identify of these peaks we need to look at the optical matrix elements \mathbf{r}_{nm} for various pairs of band n and m . We mark the transitions, giving the major structure in $\epsilon_{zz}^{(2)}(\omega)$, in the band structure plot. These transitions are labeled according to the peak labels in Fig. 2(a).

We now go on to study the NLO properties. Different contributions to the imaginary part of $\chi_{xyz}^{(2)}(2\omega, \omega, \omega)$ are presented in Fig. 2(b). As can be seen the total SHG susceptibility is zero below half the band gap. The 2ω terms start contributing at energies $\sim \frac{1}{2}E_G$ and the ω terms for energy values above E_G . In the low energy regime ($\leq 3\text{eV}$) the SHG optical spectra is dominated by the 2ω contributions. Beyond 3eV the major contribution comes from the ω terms. Unlike the linear optical spectra, the features in the SHG susceptibility are very difficult to identify from the band structure because of the complicated resonance of the 2ω and ω terms. But one can make use of the linear optical spectra to identify the different resonances leading to various features in the NLO spectra. This analysis is performed in the present work. The identified peaks are marked in Fig. 2, where the nomenclature adopted is $M(x\omega) + N(y\omega)$, which indicates that the peak comes from an $x\omega$ resonance of the peak M with the $y\omega$ resonance of peak N in the linear optical spectra. For example, the hump just below 1 eV, labeled $A(2\omega)$ in the imaginary part of $\chi_{xyz}^{(2)}(2\omega, \omega, \omega)$ comes from the 2ω resonance of the peak labeled A in the linear optical spectra. The peak labeled $D(2\omega) + B(\omega)$ is coming from the 2ω resonance of the peak D with ω resonance of the peak labeled B in the $\epsilon_2(\omega)$ plot.

Compared to the linear optical, the NLO is a much more surface/interface sensitive technique. This fact can be demonstrated by identifying the features coming from the interface formation. These features are referred to as SL features. These features can be pin pointed by comparing the spectra for the SL with features appearing from the average of the two bulk materials. In order to provide a simple model for predicting the averaged bulk features in the optical properties on basis of its constituent materials, the effective-medium-model (EMM) and the strain-corrected-effective-medium-model (SCEMM)¹⁰ have been proposed. Comparison of the SCEMM results with the SL calculations are presented in Fig. 4. The SL features coming from effects like symmetry lowering are not accounted

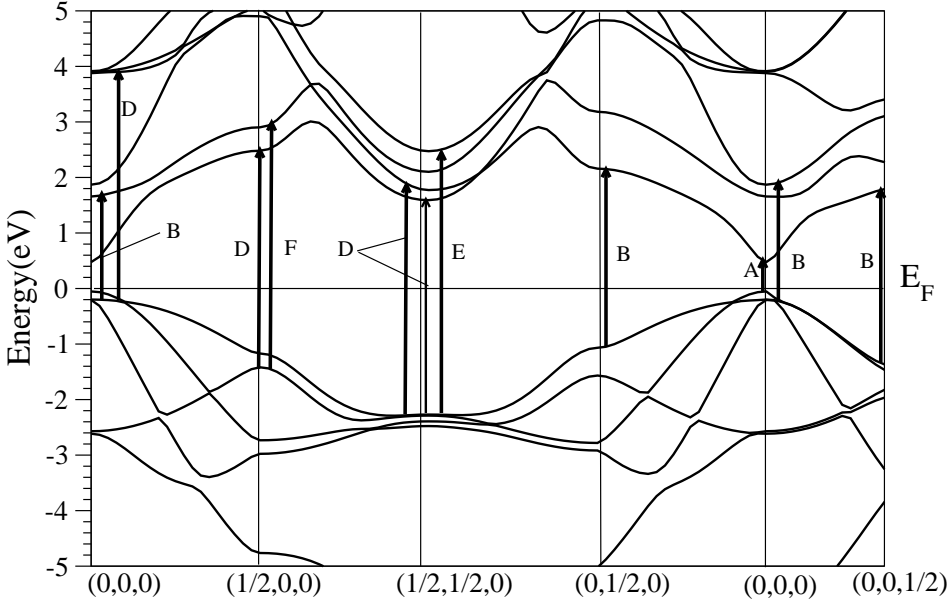


FIG. 3: Band structure for mono-layer InP/GaP SL.

for by the SCEMM and are marked as SLX in the figure, with X representing the feature label. The small SL effects in the linear optical spectra are greatly enhanced in the second-order optical response. This clearly indicates the selective interface sensitivity of the NLO.

Acknowledgements

We would like to thank the Austrian Science Fund for the financial support (projects P13430 and P16227). The code for calculating non-linear optical properties was written under the EXCITING network funded by the EU (Contract HPRN-CT-2002-00317).

* Electronic address: sangeeta.sharma@uni-graz.at

¹ Z. Q. Qiu and S. D. Bader. *Rev. Sci. Inst.*, 71:1243, 2000.

² J. L. P. Hughes and J. E. Sipe. *Phys. Rev. B*, 53:10751, 1996.

³ J. E. Sipe and Ed. Ghahramani. *Phys. Rev. B*, 48:11705, 1993.

⁴ J. E. Sipe and A. I. Shkrebtii. *Phys. Rev. B*, 61:5337, 2000.

⁵ S. N. Rashkeev, W. R. L. Lambrecht, and B. Segall. *Phys. Rev. B*, 57:3905, 1998.

⁶ T. A. Luce, W. Huebner, A. Kirilyuk, Th. Rasing, and K. H. Bennemann. *Phys. Rev. B*, 57:7377, 1998.

⁷ T. Anderson and W. Huebner. *Phys. Rev. B*, 65:174409, 2002.

⁸ U. Pustogowa, W. Huebner, and K. H. Bennemann. *Phys. Rev. B*, 48:8607, 1993.

⁹ W. Huebner and K. H. Bennemann. *Phys. Rev. B*, 40:5973, 1989.

¹⁰ S. Sharma, J. K. Dewhurst, and C. Ambrosch-Draxl. <http://xxx.lanl.gov/abs/cond-mat/0211512> (accepted for publication in PRB 2003 May issue).

¹¹ A. Franceschetti and A. Zunger. *Nature*, 402:60, 1999.

¹² C. G. Van de Walle and R. M. Martin. *Phys. Rev. B*, 34:5621, 1986.

¹³ C. G. Van de Walle and R. M. Martin. *Phys. Rev. B*, 35:8154, 1987.

¹⁴ N. Chetty A. Munoz and R. M. Martin. *Phys. Rev. B*, 41:2976, 1990.

¹⁵ B. K. Agrawal, S. Agrawal, and R. Srivastava. *Surf. Sci.*, 424:232, 1999.

¹⁶ R. G. Dandrea and A. Zunger. *Phys. Rev. B*, 43:8962, 1991.

¹⁷ Y. Tanida and M. Ikeda. *Phys. Rev. B*, 50:10958, 1994.

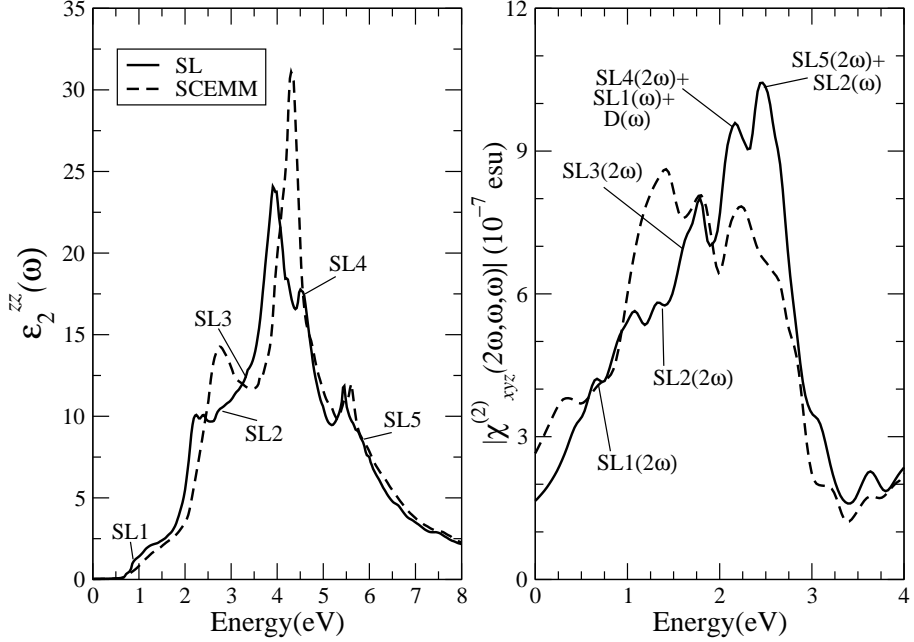


FIG. 4: Full SL calculation (solid line) along with the SCEMM results (dashed line) for (a) the imaginary part of the linear dielectric tensor and (b) the magnitude of the SHG susceptibility

- ¹⁸ C. H. Park and K. J. Chang. *Phys. Rev. B*, 47:12709, 1993.
- ¹⁹ T. Kurimoto and N. Hamada. *Phys. Rev. B*, 40:3889, 1989.
- ²⁰ J. Arriga, M. C. Munoz, V. R. Velasco, and F. Garca-Moliner. *Phys. Rev. B*, 43:9626, 1991.
- ²¹ A. Franceschetti and A. Zunger. *Appl. Phys. Lett.*, 65:2990, 1994.
- ²² Y. Kobayashi, T. Nakayama, and H. Kamimura. *J. Phys. Soc. Jpn.*, 65:3599, 1996.
- ²³ Ed. Ghahramani and J. E. Sipe. *Phys. Rev. B*, 46:1831, 1992.
- ²⁴ Ed. Ghahramani, D. J. Moss, and J. E. Sipe. *Phys. Rev. B*, 43:8990, 1991.
- ²⁵ Ed. Ghahramani, D. J. Moss, and J. E. Sipe. *Phys. Rev. B*, 41:5112, 1990.
- ²⁶ Ed. Ghahramani, D. J. Moss, and J. E. Sipe. *Phys. Rev. B*, 43:9269, 1991.
- ²⁷ The LDA is known to underestimate the bandgaps. The usual procedure is to use the scissors operator to correct the bandgap for calculating the optical response of the material. In order to keep things simple, in the present work no scissors correction is used. The scissors corrected results can be seen in the Ref. 10.